Talanta 130 (2014) 571–576

Contents lists available at ScienceDirect

Talanta

journal homepage: www.elsevier.com/locate/talanta

A fluorescent probe for the detection of Hg^{2+}: Shift from "*on-state A*" to "*on-state B*"

Priya Singla, Paramjit Kaur [*,1], Kamaljit Singh [1]

Department of Chemistry, UGC-Centre of Advanced Studies-I, Guru Nanak Dev University, Amritsar 143005, India

ARTICLE INFO

Article history:
Received 20 June 2014
Received in revised form
14 July 2014
Accepted 18 July 2014
Available online 26 July 2014

Keywords:
Pyrene based sensor
Excimer
Charge-transfer
DFT
Contact mode detection

ABSTRACT

A simple pyrene based receptor has been synthesised and shown to exist in the dimeric form in solution exhibiting an excimer band in the emission spectrum. The proposed dimeric form is supported by the DFT calculations. Further, the excimer fluorescence is bathochromically shifted with decreased emission intensity in the presence of Hg^{2+} suggestive of the formation of an aggregated complex. The sensing event also worked on the solid support; thus attesting the potential of the sensor for practical application in contact mode.

1. Introduction

Considerable strides have recently been made to design and synthesise sensor systems that present instantaneous response to heavy and transition-metal ions of prime importance for environmental and biological applications [1]. Among heavy metal ions, mercury is an extremely toxic and environmentally hazardous element which can lead to neurological, immunological, reproductive and cardiac disorders, when absorbed by the human gastrointestinal tract [2]. Its accumulation in the food chain through air, water, vaccines, cosmetic products, etc. can lead to serious health concerns [3]. The demand for Hg^{2+} sensitive probes [4–8] motivated us to investigate the applicability of simple fluorophores equipped with a binding site for soft metal ions. We have special interest in conjugated planar molecules for applications ranging from organic semiconductors to metal ion sensing [9]. We envisaged that appropriate combination of nitrogen atom binding sites might be a good choice for the recognition of soft, heavy metal ions [10]. Generally, the heavy transition metal ions are fluorescence quenchers by either enhanced spin-orbit coupling (in the case of Hg^{2+}) [11] or electron transfer (in the case of Cu^{2+}) [12] leading to turn-off detection mode. However, a turn-on/red-shifted emission signalling mode enjoys the edge as it can diminish the chances of false positive results, leading to unambiguous quantification of the binding event, especially in the biological samples [13]. The wide use and ease in structural modification of pyrene attracted our attention as an efficient fluorogenic unit [14] because of its high detection sensibility and efficiency in excimer formation leading to changes in its emission properties [15]. Fluorescence of such excimers peaks in the vicinity of 480 nm as a broad band as compared to well-structured monomer emission around 375–400 nm [16]. In some cases only the excimer like emission is observed which can be attributed to the pre-excitation association of the pyrene units and its intensity is dependent upon the extent of either the inter- or intra-molecular aggregation of pyrene monomers [17]. In the present investigation, we have found that the pyrene derivative **1** self-assembles as a dimeric unit (Scheme 1), and upon selective recognition of Hg^{2+} shows distinct optical changes.

2. Experimental

2.1. Chemicals

Pyrene, $RuCl_3 \cdot xH_2O$, and 2,3-diaminopyridine were purchased from Sigma-Aldrich. Metal salts used in the spectrophotometric studies were of analytical grade and bought from Sigma-Aldrich. For the titrations, Li^+, Na^+, Mg^{2+}, Ca^{2+}, Ba^{2+}, Mn^{2+}, Fe^{2+}, Co^{2+}, Ni^{2+}, Hg^{2+}, and Pb^{2+} were added as their perchlorates and K^+, Cu^{2+}, Zn^{2+}, Cd^{2+}, Ce^{3+}, La^{3+}, Pr^{3+}, Eu^{3+}, Nd^{3+}, Lu^{3+}, Yb^{3+}, Tb^{3+}, Sm^{3+}, and Gd^{3+} were added as their nitrates. The

* Corresponding author.
E-mail addresses: paramjit19in@yahoo.co.in (P. Kaur), kamaljit.chem@gndu.ac.in (K. Singh).
[1] Tel.: +91 183 2258853; fax: +91 183 2258819 20.

http://dx.doi.org/10.1016/j.talanta.2014.07.050
0039-9140/

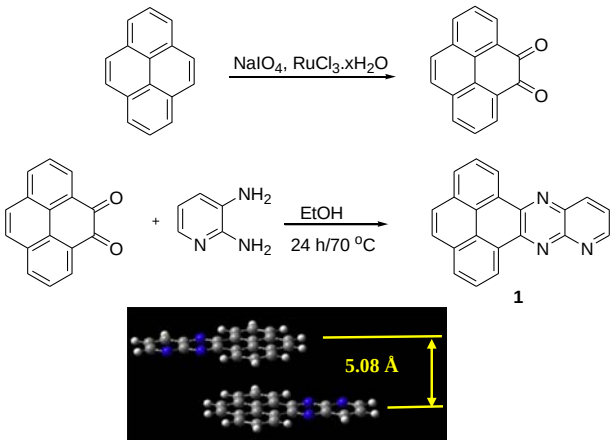

Scheme 1. Synthesis of **1**.

solvents used were of analytical grade and purchased from Thomas Baker.

2.2. Instrumentation

^{1}H NMR (300 MHz) and ^{13}C NMR (75 MHz) spectra were recorded in $CDCl_3$ on a JEOL-FT NMR-AL spectrometer. Tetramethylsilane (TMS) served as the internal standard (0 ppm for ^{1}H) and $CDCl_3$ was used as solvent. Data are reported as follows: chemical shift in ppm (δ), integration, multiplicity (s=singlet, d=doublet, m=multiplet), coupling constant J (Hz) and assignment. Mass spectra were recorded on a microTOF-Q II 10356 spectrometer. Melting points were determined in open capillaries and are uncorrected. Emission studies were made on a Perkin-Elmer LS 55 Fluorescence spectrometer with excitation slit width as 10.0 and emission slit width as 2.5 with off emission correction mode. UV–vis spectra were recorded on a SHIMADZU 1601 PC spectrophotometer, with a quartz cuvette (path length, 1 cm) and studies were performed in AR grade THF. The cell holder of the spectrophotometer was maintained at 25 °C for consistency in the recordings.

2.3. Detection limit calculations

The detection limit was calculated on the basis of the fluorescence titration. The fluorescence emission spectrum of **1** was measured 6 times, and the standard deviation of blank measurement was achieved. To gain the slope, the ratio of emission intensity at 570 nm was plotted as a concentration of Hg^{2+}. The detection limit is calculated using the following equation:

$$\text{Detection limit} = 3\sigma/K$$

where σ is the standard deviation of blank measurement, and K is the slope calculated from the ratio of emission intensity versus $[Hg^{2+}]$.

2.4. Computational details

All theoretical calculations were carried out by using the Gaussian 09 suite of programs [18]. The molecular geometry of the dimeric form of **1** was optimised at the semi-empirical level employing the PM3 functional. The same model chemistry was used for the calculation of the properties. The first 10 excited states were calculated by using time-dependent self-consistent field (TD-SCF) calculations [19]. The molecular orbital contours were plotted using Gauss view 5.0.9.

2.5. Procedure for synthesis and characterisation of **1** (Scheme 1)

2.5.1. Synthesis of pyrene-4,5-dione [20]

To a solution of pyrene (10 mmol) in CH_2Cl_2 (40.0 ml) and CH_3CN (40.0 ml) were added $NaIO_4$ (10.0 g, 46.8 mmol), H_2O (50.0 ml), and $RuCl_3 \cdot xH_2O$ (0.20 g, 0.96 mmol). The dark brown suspension was stirred at room temperature overnight. The reaction mixture was poured into 500 ml of H_2O and the organic phase was separated. The aqueous phase was extracted with CH_2Cl_2 (3×50 ml). The CH_2Cl_2 extracts were combined with the organic phase and washed with H_2O (3×200 ml) to give a dark orange solution. The solvent was removed under reduced pressure to afford a dark orange solid. Thin-layer chromatography (TLC), using an ethylacetate/hexane (2/5) mixture, indicated the presence of several byproducts, which were not isolated. Column chromatography (CH_2Cl_2) gave pure product as bright orange crystals. Yield 45%; m.p. 299–302 °C; ^{1}H NMR (300 MHz, $CDCl_3$) δ=7.78 (t, 2H, J=3.9 Hz, ArH), 7.86 (s, 2H, ArH), 8.21 (dd, 2H, J=2.7 Hz and 3.3 Hz, ArH), 8.50 (dd, 2H, J=3.9 Hz and 6.6 Hz, ArH); ^{13}C NMR (75 MHz, $CDCl_3$) δ=127.4, 128.1, 128.5, 130.20, 130.2, 132.1, 135.9, and 180.5; m/z 255.05 $[M+23]^+$.

2.5.2. Synthesis of phenanthro[4,5-fgh]pyrido[2,3-b]quinoxaline **1**

Pyrene-4,5-dione (0.500 g, 2.15 mmol) was taken in ethanol (30 ml) and the solution was refluxed for 30 min. To this hot solution of 2,3-diaminopyridine (0.230 g, 2.15 mmol) was added and the reaction mixture was allowed to reflux for overnight. At the end of the reaction, the solution was concentrated under vacuum and the crude product was filtered, washed with ethanol and dried. Pure product was obtained by recrystallising from a mixture of ethanol and di-chloromethane. Yield 47%; m.p. > 200 °C; IR (KBr pellets): υ_{max} is 3048.55 (C–H str.), 1624.96 (Ar –C=N), 1468.72 (ArC=C), 1293.19 (Ar–C–N); ^{1}H NMR (300 MHz, $CDCl_3$) δ=7.85–7.88 (m, 1H, ArH), 8.07–8.16 (m, 4H, ArH), 8.32–8.36 (m, 2H, ArH), 8.75 (d, 1H, J=8.4 Hz, ArH), 9.35 (s, 1H, ArH), 9.56 (d, 1H, J=7.8 Hz, ArH), 9.77 (d, 1H, J=7.8 Hz, ArH); m/z 306.09 $[M+1]^+$.

(For copies of the NMR, EI Mass see Figs. S1 and S2 in Supporting information).

3. Results and discussion

3.1. Synthesis

The synthesis of compound **1** (Scheme 1), began from pyrene-4,5-dione, formed from pyrene using catalytic amount of $RuCl_3 \cdot xH_2O$. Finally **1** was obtained by using standard Schiff-base condensation protocol between pyrene-4,5-dione and 2,3-diaminopyridine.

3.2. Cation-sensing studies

A solution of **1** (5×10^{-6} M, in THF) showed excimer emission at 487 nm ($\lambda_{exc.}$ 330 nm) (Fig. 1), suggesting that **1** existed in the dimeric form in solution [16]. Therefore, the theoretical calculations [18] were performed on the dimeric unit of **1**. The energy minimised structure (Scheme 1) revealed the shortest distance 5.08 Å between the molecular planes of the two pyrene units of the dimer, which is well within the range (4–10 Å) [14] for the excimer formation. The UV–visible spectrum of **1** (1×10^{-5} M, in THF) shows a broad band in the range 426–448 nm (Fig. 1) along with the typical pyrene absorption bands in the range of 312–344 nm [21]. The former, low energy broad band is assigned as the intra-ligand charge-transfer (ICT) band with contributions from HOMO-6 to LUMO+1, and from HOMO-7 to LUMO, on the basis of

the electron density distribution in the frontier molecular orbitals predicted by time dependent self-consistent field (TD-SCF) calculations (Fig. 2) (Tables S1, S2 and Fig. S3, in Supporting information).

The fluorescence behaviour of **1** (5×10^{-6} M, in THF) was explored in the presence of a number of metal ions such as Li^+, Na^+, K^+, Mg^{2+}, Ca^{2+}, Ba^{2+}, Ni^{2+}, Mn^{2+}, Co^{2+} Cu^{2+}, Zn^{2+}, Hg^{2+}, Fe^{2+}, Cr^{3+}, Al^{3+}, Yb^{3+}, La^{3+}, Eu^{3+}, Sm^{3+}, Pr^{3+}, Lu^{3+}, Ce^{3+}, Tb^{3+}, and Nd^{3+} (added as their perchlorate or nitrate salts under similar experimental conditions, 3.42×10^{-5} M, in H_2O), but a significant response was noted for Hg^{2+} ions only (Fig. 3).

We further probed the Hg^{2+} binding ability of **1**. Thus, upon addition of increasing concentrations of Hg^{2+} ions (2.8×10^{-6}–3.42×10^{-5} M, in H_2O) to the solution of **1** (5×10^{-6} M, in THF), the excimer emission band of **1** showed a bathochromic shift from 487 to 570 nm ($\Delta\lambda_{em.}=83$ nm) with an isoemissive point at 542 nm (Fig. 4a).

Such a ratiometric shift ("*on-state A*" to "*on-state B*") coupled with a decrease in emission intensity points towards the existence of (i) dimeric pyrene units and (ii) emission from only the surface molecules of the aggregate [22]. Thus, in light of these, we propose the formation of an aggregated complex in solution with the dimeric pyrene units continuing to show excimer emission.

Further, in order to strengthen the above claims, single crystal X-ray structure was analysed. Upon attempted crystallisation the complex precipitated as powder. IR analysis of this powder showed well-defined strong bands at 1095 and 621 cm^{-1} (Fig. S4, in Supporting information), attributable to the bridging perchlorate ions [23]. Crystals were obtained only after repeated attempts by heating a mixture of **1** and $Hg(ClO_4)_2\cdot xH_2O$. Indeed, the structure depicted the formation of an aggregated complex; however, it was quite surprising to note that the structure was a chloride bridged structure instead of perchlorate, the counter anion used in the binding studies.

With this interesting observations in hand, we propose that in the solution the bridged perchlorate in the initially formed aggregated complex, obtained upon heating the mixture of **1** and $Hg(ClO_4)_2\cdot xH_2O$, got reduced to chloride. Literature report [24] attests such transformation of perchlorate into chloride as perchlorate is a strong oxidising agent when heated in the presence of a Lewis base, ethanol or **1** (in the present case), and undergoes reduction to chloride due to an obvious reason of −1 oxidation

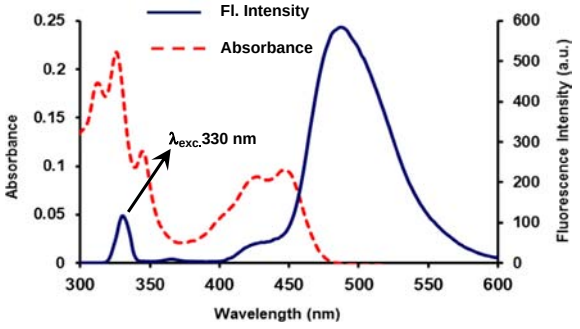

Fig. 1. Absorption (1×10^{-5} M, in THF) and emission (5×10^{-6} M, in THF) spectra of **1**.

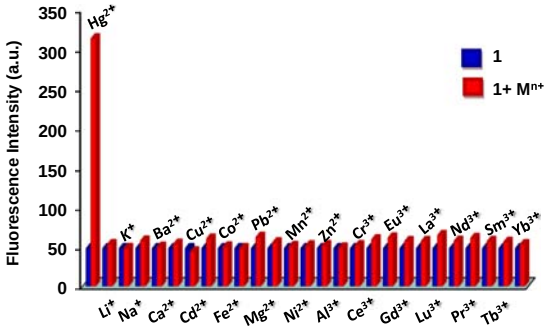

Fig. 3. Changes in the emission profile **1** (5×10^{-6} M, in THF) upon addition of different cations (3.42×10^{-5} M, in H_2O).

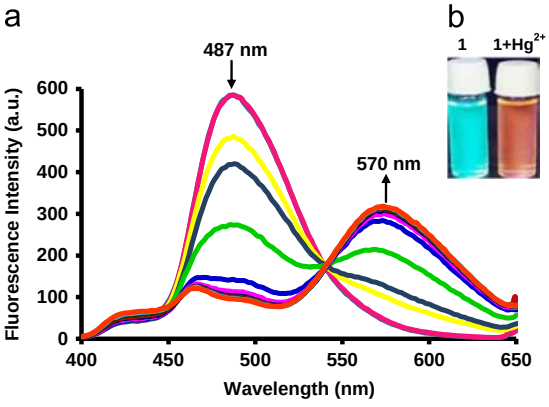

Fig. 4. (a) Changes in the emission spectra of **1** (5×10^{-6} M, in THF) upon addition of varying concentrations of Hg^{2+} (2.8×10^{-6}–3.42×10^{-5} M, in H_2O), (THF: H_2O=99:1, v/v), (b) naked-eye emission colour change upon addition of Hg^{2+}.

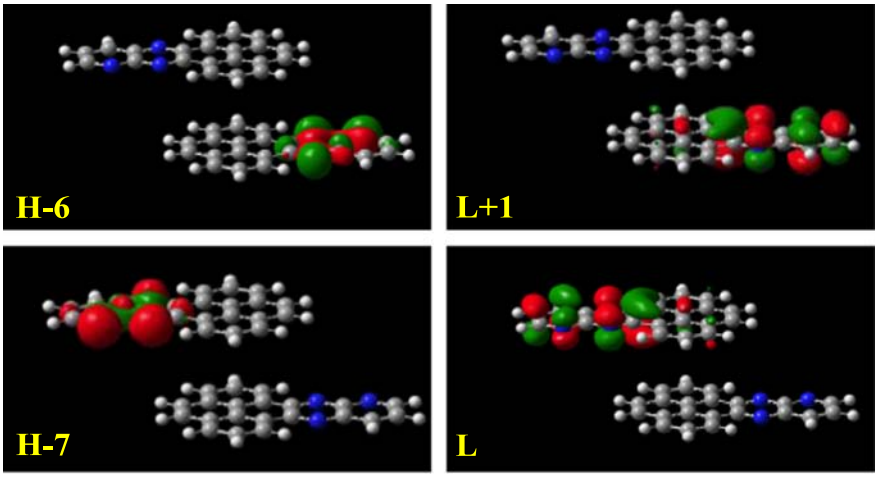

Fig. 2. Computational analysis of frontier molecular orbitals of dimeric form of **1**.

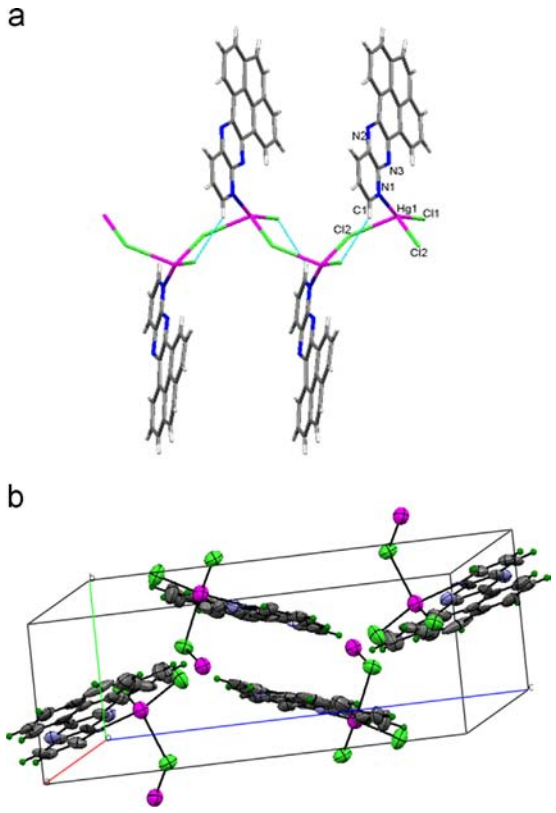

Fig. 5. (a) The preliminary single crystal X-ray structure of the chloride bridged complex depicting the excimer formation. (b) Packing diagram (CCDC 996978).

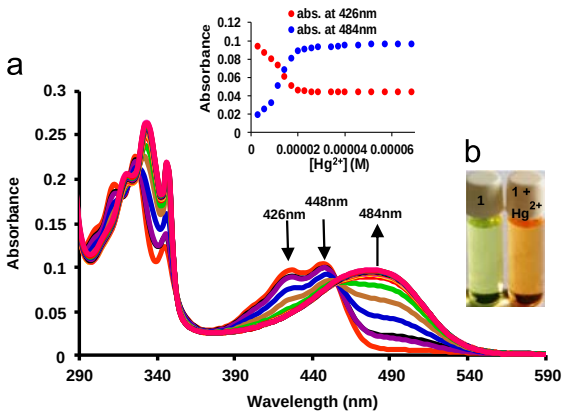

Fig. 6. Changes in the absorption spectra of **1** (1×10^{-5} M, in THF) upon addition of different concentrations of Hg^{2+} (2.8×10^{-6}–6.0×10^{-5} M, in H_2O), (THF:H_2O= 99:1, v/v). Inset: (a) Ratiometric change in absorbance at 426 nm and 484 nm, and (b) naked-eye colour change.

state being most stable one for Cl. In the chloride bridged complex as depicted in X-ray crystal structure (Fig. 5) (Table S3 and S4, in Supporting information), the coordination of Hg^{2+} is completed by a pyridyl nitrogen atom, two terminal and one bridged chlorine atoms. One of the terminal chlorine atoms attached to the Hg^{2+} ion of one unit is involved in hydrogen bonding with hydrogen atom of the –CH group adjacent to the pyridyl nitrogen atom of the other unit. Thus, the bridging and hydrogen bonded chloride ions are responsible for the formation of the aggregate.

The ICT band in the absorption spectrum of **1** (1×10^{-5} M, in THF) upon gradual addition of Hg^{2+} ions (2.8×10^{-6}–6.0×10^{-5} M, in H_2O) too exhibited the expected bathochromic shift from 426 to 484 nm ($\Delta\lambda_{abs.}$=58–36 nm) (Fig. 6), in line with the above proposal and also pointed towards the reduced energy difference in the frontier molecular orbitals on complexation with Hg^{2+}. As depicted in Fig. 2, though the HOMO and LUMOs are delocalised on the pyrido-quinoxaline unit of **1**, the LUMO is more concentrated on the pyridine site. Thus, the interaction of the guest species with this side of the chromophore **1** is expected to stabilise LUMO to a significant extent only to reduce the energy difference between HOMO and LUMO (bathochromic shift).

The observed shift in the excimer emission band from 487 to 570 nm upon binding Hg^{2+} is in stark contrast to the observed response of many pyrene based fluorophores towards metal ion binding, where the excimer emission is lost to hypsochromically shifted monomer emission [16a]. Further, the non-linear curve fitting analysis of the titration data of **1** with Hg^{2+} using HypSpec fitting programme [25] could only be successfully refined for 1:1 stoichiometric complex **1**:Hg^{2+} with the binding constant $\log\beta$=5.49. The proposed stoichiometry was further confirmed by Job's plot, a method of continuous variations, where the maximum absorption change was observed when the mole fraction of **1** versus Hg^{2+} was 0.5 (Fig. 7).

The detection limit was found to be 1.31×10^{-6} M, which is significantly better than most of the previously reported and well in the range of that exhibited by other pyrene based sensors (Table S5, in Supporting information) and was calculated from fluorescence titration spectra (Fig. S5, in supporting information). In order to ascertain whether the detection of Hg^{2+} with **1** is affected by the presence of other metal ions, competition experiments were performed. For that, when solution of Hg^{2+} (3.42×10^{-5} M, in H_2O) was added to the solution of **1** (5×10^{-6} M, in THF) in the presence of other cations (3.42×10^{-5} M, in H_2O), no interference was observed (Fig. 8).

Further, the reversibility of the binding process between **1** and Hg^{2+} was established when the original spectrum of **1** was revived upon addition of solution of cysteine (1×10^{-4} M, in

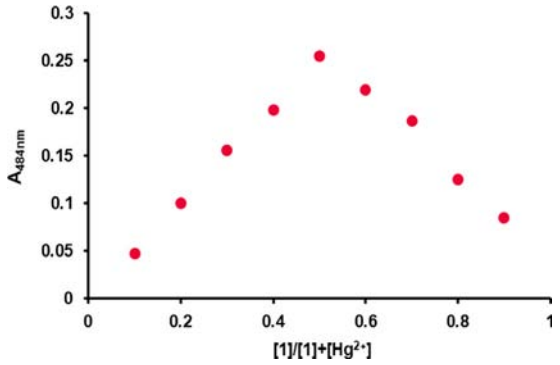

Fig. 7. Job plot of Hg^{2+} complex formation.

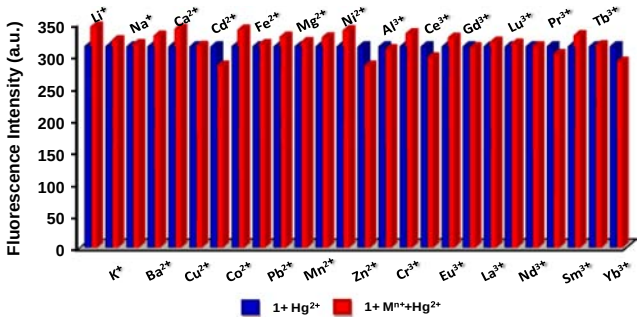

Fig. 8. Changes in the emission change of **1** (5×10^{-6} M, in THF) upon addition of Hg^{2+} (3.42×10^{-5} M, in H_2O) in the presence of other cations (3.42×10^{-5} M, in H_2O).

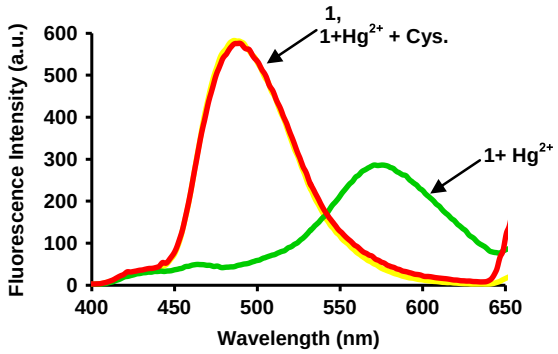

Fig. 9. Changes in the emission of **1** (5×10^{-6} M, in THF) in the presence of Hg^{2+} (3.42×10^{-5} M, in H_2O) before and after the addition of cysteine (1×10^{-4} M, in 0.1 M PBS).

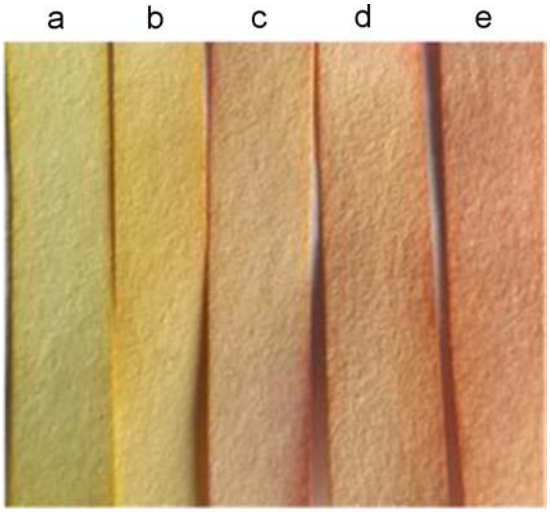

Fig. 10. Changes in the colour of the paper strips soaked with the solution of (a) **1** (5×10^{-6} M, in THF) upon treatment with the solution of Hg^{2+} ions, (b) 5×10^{-4} M, (c) 1×10^{-4} M, (d) 5×10^{-3} M and (e) 1×10^{-3} M, in H_2O.

0.1 M PBS) (Fig. 9). We also checked the sensing behaviour of pyrene and pyrene-4,5-dione towards Hg^{2+}, but no response was observed (Fig. S6, in Supporting information).

4. Practical application

Further, for the instant visual detection of Hg^{2+} without using spectroscopic instrumental methods, **1** was loaded onto paper strips. For this, Fisher brand filter paper P8, strip (4.5×0.5 cm^2) was impregnated with the solution of 1 (5×10^{-6} M, in THF) repeatedly with intermittent drying. The loaded strip thus formed was dipped in aqueous solutions of Hg^{2+} ions (5×10^{-4} M, 1×10^{-4} M, 5×10^{-3} M, and 1×10^{-3} M in H_2O) and dried in a similar way, which subsequent to the sensing led to the naked-eye colour change (Fig. 10).

5. Conclusions

In conclusion, the reported pyrene based chemosensor facilitates sensing of Hg^{2+} ions with a bathochromically shifted excimer band as a consequence of proposed perchlorate bridged aggregated complex formed in solution. The sensing event on the solid support mimics the solution sensing event; thus demonstrating potential of the chemosensor for practical applications.

Acknowledgements

The authors thank CSIR, New Delhi, India (Project: 01/2687/12-EMR-II) and Guru Nanak Dev University, Amritsar (UPE Programme) for financial assistance.

Appendix A. Supporting information

Supplementary data associated with this article can be found in the online version at http://dx.doi.org/10.1016/j.talanta.2014.07.050.

References

[1] (a) V. Amendola, L. Fabbrizzi, F. Forti, M. Licchelli, C. Mangano, P. Pallavicini, A. Poggi, D. Sacchi, A. Taglieti, Coord. Chem. Rev. 250 (2006) 273–299;
(b) J. Wu., W. Liu, J. Ge, H. Zhang, P. Wang, Chem. Soc. Rev. 40 (2011) 3483–3495.
[2] (a) W.F. Fitzgerald, C.H. Lamborg, C.R. Hammerschmidt, Chem. Rev. 107 (2007) 641–662;
(b) M. Nendza, T. Herbst, C. Kussatz, A. Gies, Chemosphere 35 (1997) 1875–1885;
(c) A. Renzoni, F. Zino, E. Franchi, Environ. Res. 77 (1998) 68–72;
(d) J.M. Llobet, G. Falco, C. Casas, A. Teixido, J.L. Damingo, J. Agric. Food Chem. 51 (2003) 838–842.
[3] (a) M.Q. Zhang, Y.C. Zhu, R.W. Deng, China AMBIO 31 (2002) 482–484;
(b) G. Westphal, E. Hallier, Lancet 361 (2003) 698–699;
(c) M. Harada, S. Nakachi, K. Tasaka, S. Sakashita, K. Muta, K. Yanagida, R. Doi, T. Kazaki, H. Ohno, Sci. Total Environ. 269 (2001) 183–187.
[4] W. Lu, X. Qin, S. Liu, G. Chang, Y. Zhang, Y. Luo, A.M. Asiri, A.O.A. Youbi, X. Sun, Anal. Chem. 84 (2012) 5351–5357.
[5] L. Wang, J. Tian, H. Li, Y. Zhang, X. Sun, J. Fluoresc. 21 (2011) 1049–1052.
[6] H. Li, J. Zhaia, J. Tiana, Y. Luoa, X. Suna, Biosens. Bioelectron. 26 (2011) 4656–4660.
[7] H. Li, J. Zhai, X. Sun, Nanoscale 3 (2011) 2155–2157.
[8] S. Liua, X. Qina, J. Tiana, L. Wanga, X. Suna, Sens. Actuat. B 171–172 (2012) 886–890.
[9] (a) P. Kaur, D. Sareen, Dyes Pigment. 88 (2011) 296–300;
(b) P. Kaur, D. Sareen, K. Singh, Talanta 83 (2011) 1695–1700;
(c) P. Kaur, D. Sareen, K. Singh, Dalton Trans. 41 (2012) 8767–8769;
(d) P. Kaur, D. Sareen, K. Singh, Anal. Chim. Acta 778 (2013) 79–86;
(e) P. Kaur, S. Kaur, Y. Kasetti, P.V. Bharatam, K. Singh, Talanta 83 (2010) 644–650.
[10] (a) K. Rurack, U. Resch-Genger, J.L. Bricks, M. Spieles, Chem. Commun. (2000) 2103–2104;
(b) R.N. Cha, M.Y. Kim, Y.H. Kim, J.L. Choe, S.F. Chang, J. Chem. Soc., Perkin Trans. 2 (2002) 1193–1196.
[11] D.S.M. Clure, J. Chem. Phys. 20 (1952) 682–686.
[12] K. Rurack, V. Resch, M. Senoner, S. Dachne, J. Fluoresc. 3 (1993) 141–143.
[13] (a) S.C. Burdette, S.J. Lippard, J. Inorg. Chem 41 (2002) 6816–6823;
(b) M. Taki, J.L. Wolford, T.V. Halloran, J. Am. Chem. Soc. 126 (2004) 712–713.
[14] F.M. Winnick, Chem. Rev. 93 (1993) 587–614.
[15] (a) S. Nishizawa, A. Kato, N. Teramae, J. Am. Chem. Soc. 121 (1999) 9463–9464;
(b) D. Sahoo, V. Narayanswami, C.M. Kay, R.O. Ryan, Biochemistry 39 (2000) 6594–6601;
(c) J.B. Birks, Photophysics of Aromatic Molecules, 74, Wiley-Interscience, London (1970) 1294–1295.
[16] (a) J.S. Kim, D.T. Quang, Chem. Rev. 107 (2007) 3780–3799;
(b) H.J. Kim, M.H. Lee, L. Mutihac, J. Vicens, J.S. Kim, Chem. Soc. Rev. 41 (2012) 1173–1190;
(c) D.T. Quang, J.S. Kim, Chem. Rev. 110 (2010) 6280–6301.
[17] J. Cho, T. Pradhan, J.S. Kim, S. Kim, Org. Lett. 15 (2013) 4058–4061.
[18] M.J. Frisch, G.W. Trucks, H.B. Schlegel, G.E. Scuseria, M.A. Robb, J.R. Cheeseman, G. Scalmani, V. Barone, B. Mennucci, G.A. Petersson, H. Nakatsuji, M. Caricato, X. Li, H.P. Hratchian, A.F. Izmaylov, J. Bloino, G. Zheng, J.L. Sonnenberg, M. Hada, M. Ehara, K. Toyota, R. Fukuda, J. Hasegawa, M. Ishida, T. Nakajima, Y. Honda, O. Kitao, H. Nakai, T. Vreven, J.A. Montgomery, Jr., J.E. Peralta, F. Ogliaro, M. Bearpark, J. J. Heyd, E. Brothers, K.N. Kudin, V.N. Staroverov, T. Keith, R. Kobayashi, J. Normand, K. Raghavachari, A. Rendell, J.C. Burant, S.S. Iyengar, J. Tomasi, M. Cossi, N. Rega, J. M. Millam, M. Klene, J.E. Knox, J.B. Cross, V. Bakken, C. Adamo, J. Jaramillo, R. Gomperts, R.E. Stratmann, O. Yazyev, A.J. Austin, R. Cammi, C. Pomelli, J.W. Ochterski, R.L. Martin, K. Morokuma, V.G. Zakrzewski, G.A. Voth, P. Salvador, J.J. Dannenberg, S. Dapprich, A.D. Daniels, O. Farkas, J.B. Foresman, J.V. Ortiz, J. Cioslowski, D.J. Fox, Gaussian 09, Revision B.01, Gaussian, Inc., Wallingford CT, 2010.

[19] (a) R.B. Gerber, V. Buch, M.A. Ratner, J. Chem. Phys. 77 (1982) 3022–3030;
(b) V. Buch, R.B. Gerber, M.A. Ratner, Chem. Phys. Lett. 101 (1983) 44–48;
(c) R.B. Gerber, V. Buch, M.A. Ratner, Chem. Phys. Lett. 91 (1982) 173–177;
(d) G.C. Schatz, V. Buch, M.A. Ratner, J. Chem. Phys. 79 (1983) 1808–1822.
[20] J.H.D. Zhang, F.W. Harri, J. Org. Chem. 70 (2005) 707–708.
[21] R. Martinez, A. Espinosa, A. Terraga, P. Molina, Org. Lett. 7 (2005) 5869–5872.
[22] (a) J. Liang, Z. Chen, J. Yin, A.C. Yu, S.H. Liu, Chem. Commun. 49 (2013) 3567–3569;
(b) X. Zhang, Z. Chi, B. Xu, C. Chen, X. Zhou, Y. Zhang, S. Li, J. Xu, J. Mater. Chem. 22 (2012) 18505–18513.
[23] W. Chen, M. Du, X.-H. Bu, R.-H. Zhang, T.C.W. Mak, CrystEngComm 5 (2003) 96–100.
[24] F.A. Cotton, G. Wilkinson, Advanced Inorganic Chemistry, John Wiley and Sons, New York, 1988.
[25] P. Gans, A. Sabatini, A. Vacca, Talanta 43 (1996) 1739–1753.